Multiple Trellis Coded Frequency and Phase Modulation

Shalini S. Periyalwar and Solomon M. Fleisher, *Senior Member, IEEE*

Abstract—**Multiple trellis coded modulation of constant envelope frequency and phase modulated signal sets (MTCM/FPM) is investigated for performance on the AWGN channel and on the one-sided normal, Rayleigh- and Rician-fading channels. The Nakagami-m fading model is used as an alternative to the Rician-fading model to calculate the error probability upper bound for trellis coded schemes on the fading channel. The likenesses and the disparity between the upper bounds to the error probability for the two fading models is discussed. The design criteria for the one-sided normal fading channel, modeled by the Nakagami-m distribution, are observed to be the same as those for the Rayleigh-fading channel. For the MTCM/FPM schemes considered in this study, it is demonstrated that the set partitioning designed to maximize symbol diversity (optimum for fading channels) is optimum for performance on the AWGN channel as well. The MTCM/FPM schemes demonstrate improved performance over MTCM/MPSK schemes and TCM/FPM schemes on the AWGN channel and the fading channel. The simultaneous optimization of set partitioning rules for AWGN and fading channels proves to be particularly advantageous for the Rician-fading channels with less severe fading conditions.**

I. Introduction

TRELLIS coding using multidimensional signal sets has been extensively investigated. Multidimensional trellis codes with lattice type signal constellations have been analyzed for performance on the AWGN channel by Ungerboeck [1], Forney [2], Wei [3], and others. The advantages that accrue from the use of these codes on the AWGN channel are modest coding gains and decreased sensitivity to phase jitter, but these advantages are also accompanied by an increase in the error coefficient. The use of multidimensional signal sets also allows the transmission of non-integer number of bits per symbol.

Multidimensional modulations may be realized by the transmission of a sequence of constituent 1-D or 2-D symbols. Thus, for example, 4-D and 8-D modulations are obtained from 2-D modulations by the transmission of groups of 2 or 4 symbols. By applying this technique to trellis coding of M-ary PSK and M-ary AM signal sets, Divsalar and Simon introduced the concept of multiple trellis coded modulation (MTCM) [4]. In a sequence of papers on the subject, the authors have extensively investigated the performance of MTCM on the AWGN channel [4], [7], and on the fading channel [5], [6].

The basic MTCM encoder-modulator [4] consists of a rate b/s convolutional encoder, and a memoryless mapper-modulator scheme. The number of bits s out of the encoder is related to the multiplicity k of the MTCM scheme as $s = k \log_2 M$. The s output bits are mapped into k M-ary output symbols selected from an expanded signal set. The thourghput of the MTCM scheme is b/k bps/Hz. The trellis structure consists of 2^b transitions from each state in the trellis diagram, with each transition being represented by k M-ary symbols, chosen in such a way as to meet the code design and set partitioning criteria. Thus, 2^{b+1} distinct k-tuples of M-ary symbols are required.

On the AWGN channel, the superiority of MTCM/MPSK over conventional[1] TCM/MPSK, has been demonstrated for *two-state* trellis codes transmitting two symbols per trellis branch [4], and for higher number of states when more than two symbols per trellis branch are transmitted [7]. The performance gains obtained by MTCM/MPSK on the fading channel is illustrated by several examples in [6].

It is well known that the design criterion for trellis codes on the AWGN channel is the maximization of d^2(free). On the Rayleigh fading channel, under the conditions of ideal interleaving/deinterleaving, the criteria for optimum code design are the *length* $L_{\min}$ (defined as the number of symbols at nonzero Euclidean distance) of the shortest error event path, and the *product* of branch distances P along that path [5]. On the Rician-fading channel with stronger direct signal components, the performance is affected by all three quantities mentioned above (d^2(free), $L_{\min}$, and P). Hence, a code design and set partitioning technique optimum for the general Rician-fading channel must simultaneously satisfy the *length* and branch distance *product* criteria, and the d^2(free) criterion. MTCM schemes transmitting multiple signals per trellis branch, provide the freedom to design codes with larger values of $L_{\min}$ than that obtainable with TCM schemes. Two different set partitioning techniques have been proposed for MTCM/MPSK, to meet the code design criteria for the AWGN channel and the Rayleigh-fading channel [5]. With these set partitioning techniques, all the criteria mentioned above cannot be met simultaneously, and set partitioning based on meeting the maximum $L_{\min}$ and P criteria leads to d^2(free) lower than that obtained by using set partitioning optimum for the AWGN channel [6]. Hence, these partitioning techniques applied to

Paper approved by the Editor for Modulation Theory and Nonlinear Channels of the IEEE Communications Society. Manuscript received December 7, 1989; revised December 17, 1990. This work was supported in part by the National Science and Engineering Research Council (NSERC) of Canada, under Grant NSERC 9472. This paper was presented in part at the 1989 IEEE Pacific Rim Conference on Communications, Computers and Signal Processing, June 1–2, 1989, Victoria B.C., Canada.

The authors are with the Department of Electrical Engineering, Technical University of Nova Scotia, Halifax NS B3J 2X4, Canada.

IEEE Log Number 9108049.

[1]The term *conventional* TCM refers to the original scheme of Ungerboeck [8].

M-ary PSK are not optimum for the general Rician-fading channel.

It turns out, however, that the criteria are met simultaneously when the multiple trellis code design rules optimum for the Rayleigh-fading channel are applied to a different signal set—the combined frequency and phase modulated (FPM) signal set. Conventional trellis coding of constant envelope M-ary signals employing frequency and phase modulation (TCM/FPM) (e.g., 2FSK/MPSK, 4FSK/MPSK) has been discussed by Padovani and Wolf [10] with application to the AWGN channel. The symbols constituting the FPM signal set for the 2FSK/MPSK schemes discussed in this paper are defined by [10, eq.(5)]

$$s(t) = \sqrt{\frac{2}{T}}\ \cos[(\omega_c \pm h\pi/T)t - \phi_i] \tag{1}$$

where T is the symbol duration, and $\phi_i \in (0, 2\pi/M, \cdots, 2\cdot(M-1)\pi/M)$ for 2FSK/MPSK schemes. The two FSK frequencies are defined by $(\omega_c + h\pi/T)$ and $(\omega_c - h\pi/T)$ rad/s, with h as the modulation index. The signal space is four dimensional, and is defined in [10].

In this paper, MTCM of FPM signals (MTCM/FPM) is investigated for performance on the AWGN channel, and on the one-sided normal, Rayleigh- and Rician-fading channels. It is shown that MTCM/FPM provides improved performance compared to both TCM/FPM and MTCM/MPSK schemes. The performance of trellis coded schemes on the fading channel modeled by the Nakagami-m distribution is also analyzed. The Nakagami-m distribution has been suggested as an approximation[2] of the Rician distribution for the fading channel [11], [14]. In this paper, the Nakagami-m fading model is utilized for two reasons: it includes the one-sided normal fading model corresponding to the value $m = 1/2$, and the simple expression for the upper bound on the error probability can be used to assess the likenesses and disparities between the two fading channel models. In Section II of this paper the error probability bound for trellis coded schemes on the Nakagami-m fading channel is derived, and is compared with the error probability bound for the Rician-fading channel derived in [5]. Full interleaving (zero memory) and coherent detection with ideal channel state information are assumed. Section III covers the performance analysis of multiple trellis coded FPM signals on the AWGN channel, and on the one-sided normal, Rayleigh- and Rician-fading channels. Section IV contains the discussion.

II. Error Probability Bound for MTCM/MPSK and MTCM/FPM Schemes on the Nakagami-m Fading Channel

The performance analysis of trellis coded MPSK schemes on the Rician-fading channel is discussed in [5], from which code design criteria for optimum performance on the Rayleigh-fading channel [6], under the conditions of ideal interleaving/deinterleaving and high SNR, follow. In this section, the performance upper bound is derived for constant envelope trellis coded schemes such as MTCM/MPSK and MTCM/FPM using the Nakagami-m distribution and compared with the results for the Rician distribution.

[2]Shortly, we shall show the limited conditions under which this approximation is valid from the standpoint of error probability calculations.

The average bit error probability for trellis coded signals is upper bounded by the union bound [5]

$$P_b \le \sum_{x} \sum_{\hat{x} \in C} N(\boldsymbol{x}, \hat{\boldsymbol{x}}) p(\boldsymbol{x}) P(\boldsymbol{x} \to \hat{\boldsymbol{x}}) \tag{2}$$

where $\boldsymbol{x}$ and $\hat{\boldsymbol{x}}$ denote the transmitted and decoded sequences that belong to the set C of codeword sequences, respectively; $p(\boldsymbol{x})$ denotes the *a priori* probability of transmitting the sequence $\boldsymbol{x}$; and $P(\boldsymbol{x} \to \hat{\boldsymbol{x}})$ denotes the pairwise error probability. The performance analysis will be restricted to studying the effect of fading on the amplitude of the received signal, with the assumption that the phase and the frequency recovery is perfect.

On the fading channel, the pairwise error probability is conditioned on the fading amplitude vector $\boldsymbol{\rho} = (\rho_1, \rho_2, \cdots, \rho_l, \cdots, \rho_n)$, and is upper bounded as

$$P(\boldsymbol{x} \to \hat{\boldsymbol{x}} | \boldsymbol{\rho}) \le \exp\left(- \frac{E_s}{4N_0} \sum_{l=1}^{L} \rho_l^2 |x_l - \hat{x}_l|^2 \right) \int \tag{3}$$

where ρ_l is the normalized fading amplitude for the lth transmission interval, and L is the length of the error sequence $\hat{\boldsymbol{x}} \neq \boldsymbol{x}$. Equation (3) holds under the assumptions of ideal interleaving/deinterleaving, coherent detection with perfect channel state information, and a Gaussian decoding metric [12].

The fading amplitude of each received channel symbol is described by the Nakagami-m-distribution as

$$p(\rho) = \frac{2m^m \rho^{2m-1}}{\Gamma(m)\Omega^m} \exp[-(m/\Omega)\rho^2] \qquad \rho \ge 0 \tag{4}$$

where $\Omega = \overline{\rho^2} = 1$ under normalized conditions, $\Gamma(.)$ is the gamma-function, and

$$m = \frac{\left(\overline{\rho^2}\right)^2}{\left(\rho^2 - \overline{\rho^2}\right)^2} \ge 1/2 . \tag{5}$$

The pairwise error probability on the Nakagami-m fading channel is calculated using (3) and (4), as follows:

$$P(\boldsymbol{x} \to \hat{\boldsymbol{x}}) \le \prod_{l=1}^{L} \int_0^{\infty} \frac{2m^m \rho_l^{2m-1} e^{-m\rho_l^2}}{\Gamma(m)} \cdot \exp\left(- \frac{E_s}{4N_0} \rho_l^2 |x_l - \hat{x}_l|^2 \right) d\rho_l. \tag{6}$$

Letting $t = m\rho_l^2$ and $\alpha = 1 + \frac{E_s}{4mN_0} |x_l - \hat{x}_l|^2$

$$P(\boldsymbol{x} \to \hat{\boldsymbol{x}}) \le \prod_{l=1}^{L} \int_0^{\infty} \frac{t^{m-1} e^{-\alpha t}}{\Gamma(m)}\, dt. \tag{7}$$

By [13, 3.381(4))], (7) reduces to

$$P(\boldsymbol{x} \to \hat{\boldsymbol{x}}) \le \prod_{l=1}^{L} \left(1 + \frac{\overline{E}_s}{4mN_0} |x_l - \hat{x}_l|^2 \right)^{-m} \tag{8}$$

with the overbar denoting averaging. Equation (8) can be written in the familiar form

$$P(\boldsymbol{x} \to \hat{\boldsymbol{x}}) \le \exp\left(-\frac{\overline{E}_s}{4N_0} d^2\right) \tag{9}$$

where $d^2 = \sum_{l=1}^{L} d_l^2$, with d_l^2 defined as

$$d_l^2 = \left(\frac{\overline{E}_s}{4N_0}\right)^{-1} \ln\left(1 + \frac{\overline{E}_s}{4mN_0} |x_l - \hat{x}_l|^2\right)^m. \tag{10}$$

From the analysis in [5], it can be seen that d^2 satisfies the conditions for a distance metric.

In the case of the one-sided normal fading ($m = 1/2$), and at a high SNR, (8) reduces to

$$P(\boldsymbol{x} \to \hat{\boldsymbol{x}}) \le \prod_{l=1}^{L} \left(\frac{\overline{E}_s}{2N_0} |x_l - \hat{x}_l|^2\right)^{-1/2} \tag{11}$$

From (11), one may observe that $P(\boldsymbol{x} \to \hat{\boldsymbol{x}})$ varies as the inverse of the product of the square root of $\overline{E}_s/N_0$ and the roots of the squared Euclidean branch distances along the error event path. Therefore, the design criteria for the one-sided normal fading channel are the signal diversity and the product of branch distances (the same as those for the Rayleigh fading channel [5]).

For $m = 1$ (Rayleigh fading), (10) evaluates to

$$d_l^2 = \left(\frac{\overline{E}_s}{4N_0}\right)^{-1} \ln\left(1 + \frac{\overline{E}_s}{4N_0} |x_l - \hat{x}_l|^2\right) \tag{12}$$

which is the same result as in [5, eq. (6b)]. Under high SNR conditions with Rayleigh fading (8) evaluates to

$$P(\boldsymbol{x} \to \hat{\boldsymbol{x}}) \le \prod_{l=1}^{L} \left(\frac{\overline{E}_s}{4N_0} |x_l - \hat{x}_l|^2\right)^{-1}, \tag{13}$$

i.e., the same result as in [5, eq. (7)]. The pairwise error probability is now observed to vary as the inverse of the product of $\overline{E}_s/N_0$ and the squared Euclidean branch distances along the error event path.

In order to show that (8) can also be used to represent the performance on the AWGN channel ($m = \infty$), we rewrite (8) as

$$P(\boldsymbol{x} \to \hat{\boldsymbol{x}}) \le \prod_{l=1}^{L} (1 + y)^{-\beta/y} \tag{14}$$

where $y = \beta/m$, and $\beta = \frac{\overline{E}_s}{4N_0} |x_l - \hat{x}_l|^2$. By using the identity $\lim_{y \to 0} (1 + y)^{1/y} = e$, (14) reduces to

$$P(\boldsymbol{x} \to \hat{\boldsymbol{x}}) \le \prod_{l=1}^{L} \exp\left(-\frac{\overline{E}_s}{4N_0} |x_l - \hat{x}_l|^2\right). \tag{15}$$

Again, comparing (15) to (9), $d^2 = \sum_{l=1}^{L} d_l^2$ and

$$d_l^2 = |x_l - \hat{x}_l|^2. \tag{16}$$

Hence, d^2 is now the sum of the squared Euclidean distances along the error event path, which is the appropriate result for the AWGN channel.

Finally, (8) may be substituted in (2) to yield

$$P_b \le \sum_{x} \sum_{\hat{x} \in C} N(\boldsymbol{x}, \hat{\boldsymbol{x}}) p(\boldsymbol{x}) \cdot \prod_{l=1}^{L} \left(1 + \frac{\overline{E}_s}{4mN_0} |x_l - \hat{x}_l|^2\right)^{-m}. \tag{17}$$

For $m \ge 1$, the Nakagami-m distribution is considered by some [11], [14] as an approximation to the Rician distribution which is described as

$$p(\rho) = \frac{\rho}{\sigma^2} \exp(-\gamma) \exp\left(-\frac{\rho^2}{2\sigma^2}\right) I_0\left(\frac{2\gamma\rho^2}{\sigma^2}\right)^{1/2} \tag{18}$$

where γ is the ratio of the power in the scattered (fading) component to the power in the direct (specular) component. Here, $\gamma = 0$ corresponds to the Rayleigh fading, and $\gamma = \infty$ describes the AWGN channel. For "equivalence" between (4) and (18), the values m and γ are related by [11]

$$\gamma = \frac{(m^2 - m)^{1/2}}{m - (m^2 - m)^{1/2}} \quad m \ge 1. \tag{19}$$

The equivalence is exact for $m = 1 (\gamma = 0)$ and $m = \infty$ $(\gamma = \infty)$ only. This is also apparent from the results in (13) and (15) which are the same as those obtained using the limiting cases of the Rician distribution in [5].

For intermediate values of m, (8) has to be examined further. For fixed m and sufficiently large $\overline{E}_s/N_0$, (8) asymptotically becomes

$$P(\boldsymbol{x} \to \hat{\boldsymbol{x}}) \le \frac{(m)^{mL}}{\left(\frac{\overline{E}_s}{4N_0}\right)^{mL}} \prod_{l=1}^{L} |x_l - \hat{x}_l|^{-2m}. \tag{20}$$

Then, at high SNR, the pairwise error probability varies inversely with $(\overline{E}_s/N_0)^{mL}$. This implies that the effective diversity is the product of m (due to the channel) and L (due to the code). Compare (20) to the asymptotic expression for the Rician-fading channel [5]

$$P(\boldsymbol{x} \to \hat{\boldsymbol{x}}) \le \frac{(1 + \gamma)^L e^{-\gamma K}}{\left(\frac{\overline{E}_s}{4N_0}\right)^L} \prod_{l=1}^{L} |x_l - \hat{x}_l|^{-2} \tag{21}$$

in which the effective diversity is equal to L. It is clear that the Rician channel does not contribute a diversity of its own, as opposed to the Nakagami-m channel. This causes a discrepancy between the error probabilities for the two types of channels for $1 < m < \infty$. The approximation is close only at low SNR's, but becomes increasingly disparate as the SNR increases. This was also revealed by the numerical computation of the pairwise error probability bound given by (8) and [5, eq. (4)], for the two types of channels, respectively.

The difference between the two fading models which have been suggested to be equivalent in literature, was first shown by Crepeau [14] in the performance analysis of block-coded noncoherent FSK.

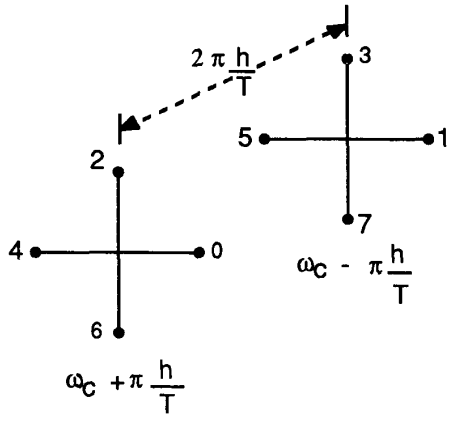

Fig. 1. The 2FSK/4PSK signal set sketched as a pair of two-dimensional 4PSK signal sets at frequencies $\omega_c + h\pi/T$ and $\omega_c - h\pi/T$ rad/s. Squared Euclidean distances between signal points for selected values of h and ϕ are listed in Table I.

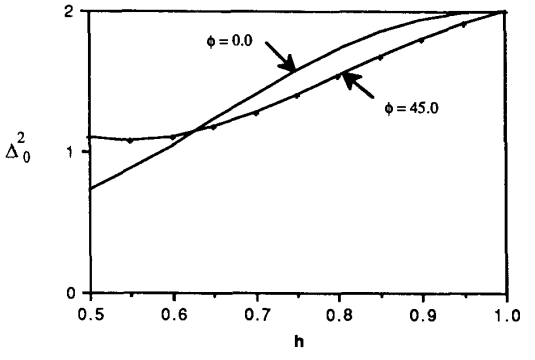

Fig. 2. Δ_0^2 versus h for the 2FSK/4PSK signal set.

III. MTCM/FPM: Performance Analysis

In this section, MTCM/FPM schemes (with $k = 2$) are investigated for performance on the AWGN channel and the fading channels. The MTCM/(2FSK/4PSK) scheme is investigated in detail, while the MTCM/(2FSK/8PSK) scheme is discussed briefly at the end of this section.

A. MTCM/(2FSK/4PSK)

The 2FSK/4PSK signal set, used in conjunction with the rate 4/6 trellis encoder, is shown in Fig. 1 as two 4PSK signal sets separated in frequency by $\Delta\omega = 2\pi\frac{h}{T}$, where T is the symbol interval. The minimum squared Euclidean distance Δ_0^2 between the odd and even numbered signal points in an MPSK signal set depends only on M, whereas in a 2FSK/4PSK signal set, Δ_0^2 is also a function of h and the phase shift between the two 4PSK constellations. The dependence of Δ_0^2 versus h for phase shifts of 0° and 45° is depicted in Fig. 2 [10]. For any other value of ϕ, Δ_0^2 lies between the values for these two curves. Note that the value of Δ_0^2 does not increase indefinitely with increasing h. The maximum value of Δ_0^2 equal to 2.0 is obtained for $h = 1.0$.

Table I contains the squared Euclidean distances between the signal points and the values of Δ_0^2, for the 8PSK signal set, and for the 2FSK/4PSK signal set for selected values of h and phase shift ϕ (a unit radius is assumed for the PSK constellations).

TABLE I
Squared Euclidean Distances Between Signal Points in the 2FSK/4PSK Signal Set and in the 8PSK Signal Set

	2FSK/4PSK				8PSK
	$h = 0.25$ $\phi = 0°$	$h = 0.5$ $\phi = 45°$	$h = 0.75$ $\phi = 0°$	$h = 1.0$ $\phi = 0°$	
$d^2(0,1)$	3.2733	1.0997	2.4244	2.0	0.5876
$d^2(0,3)$	3.2773	2.9003	2.4244	2.0	3.4124
$d^2(0,5)$	0.7269	2.9003	1.5756	2.0	3.4124
$d^2(0,7)$	0.7269	1.0997	1.5756	2.0	0.5876
Δ_0^2	0.7269	1.0997	1.5756	2.0	0.5876

First, let us illustrate the set partitioning for MTCM/MPSK for optimum performance on the AWGN channel [7] and on the fading channel [5], for an 8-ary scheme. In accordance with the Cartesian set product technique [1], let $A0$ denote the complete 8-ary signal set, and let $A0 \times A0$, denoting a two-fold Cartesian product of $A0$ with itself, be the source set.

The source set of 64 elements can be partitioned into subsets in accordance with the required performance criteria. Following [5], in the case of MTCM/MPSK, subsets should be chosen from the source set to meet the criterion of maximum $d^2(\text{free})$ on the AWGN channel, and for the fading channel, subsets are chosen to maximize the *length* $L_{\min}$ and the branch distance *product* P along the error event path. The latter partition rule is asymptotically (large SNR) optimum not only for the Rayleigh-fading channel, but for the one-sided normal fading channel as well, since it follows from (11) that the design criteria for both channels are the same. These set partition rules applied to a two-state trellis with eight parallel branches are illustrated in Fig. 3, where Set Partition I (SP-I) is the design optimum for the AWGN channel, and Set Partition II (SP-II) is the design for the fading channel, that maximizes $L_{\min}$ and P.

However, as stated in the introduction, neither of these partitions are optimum for MTCM/MPSK in the case of Rician fading ($0 < \gamma < \infty$). While it has been shown [6] that SP-II yields a lower value of $d^2(\text{free})$ than SP-I, note that SP-I yields a lower value of $L_{\min}(= 1)$ than SP-II, which has $L_{\min} = 2$. It will be shown, however, that when applied to MTCM/FPM, SP-II is optimum for both the AWGN channel and the fading channel, in the sense that all three design criteria (maximum $d^2(\text{free})$ $L_{\min}$ and P) are met simultaneously. To demonstrate this, the performances of the MTCM/8PSK scheme and the MTCM/(2FSK/4PSK) scheme are evaluated in terms of $d^2(\text{free})$ with both designs. If $d^2(\text{free})$ is larger or the same with SP-II when compared to SP-I, it may be concluded that SP-II is asymptotically optimum on both the AWGN and the fading channel; in the opposite case, two separate designs are needed–SP-I for the AWGN channel, and SP-II for the fading channel.

The values of $d^2(\text{free})$ in terms of Δ_0^2 are listed in Table II, for various numbers of states. Referring to Fig. 3, for a two-

TABLE II
SQUARED EUCLIDEAN DISTANCES IN TERMS OF Δ_0^2 FOR THE ONE-BRANCH AND TWO-BRANCH ERROR EVENTS USING SET PARTITIONING I (SP-I) AND SET-PARTITIONING II (SP-II)

Set Partition I					
No. of states	d_1^2	d_2^2 $\Delta_0^2 < 1$	d^2(free) 8PSK	d_2^2 $\Delta_0^2 \geq 1$	$d^2(\text{free}) = \min(d_1^2, d_2^2)\|_{\Delta_0^2=2}$ 2FSK/4PSK ($h = 1.0$, $\phi = 0$)
2	4	$2 + 2\Delta_0^2$	3.17	$2 + 2\Delta_0^2$	4.0
4	4	$2 + 2\Delta_0^2$	3.17	$2 + 2\Delta_0^2$	4.0
8	8	$2 + 2\Delta_0^2$	3.17	$2 + 2\Delta_0^2$	6.0
16_{HC}	8	$4 + 2\Delta_0^2$	5.17	$2 + 4$	6.0
Set Partition II					
No. of states	d_1^2	d_2^2 $\Delta_0^2 < 1$	d^2(free) 8PSK	d_2^2 $\Delta_0^2 \geq 1$	$d^2(\text{free}) = \min(d_1^2, d_2^2)\|_{\Delta_0^2=2}$ 2FSK/4PSK ($h = 1.0$, $\phi = 0$)
2	4	$4\Delta_0^2$	2.34	$2 + 2\Delta_0^2$	4.0
4	4	$4\Delta_0^2$	2.34	$2 + 2\Delta_0^2$	4.0
8	8	$4\Delta_0^2$	2.34	$2 + 2\Delta_0^2$	6.0
16_{HC}[a]	8	$6\Delta_0^2$	3.51	$4 + 2\Delta_0^2$	8.0

[a]HC—Half-connected.

state trellis, the minimum squared distance for an error event along the one-branch parallel path ($k = 2$) is $d^2_{1(\text{SP-I})} = d^2_{1(\text{SP-II})} = 4.0$ for both schemes. For the two-branch error event path, the minimum squared distance is influenced by the inter-subset distances which depend on the value of Δ_0^2 : $d^2_{2(\text{SP-I})} = 2 + 2\Delta_0^2$, and $d^2_{2(\text{SP-II})} = 4\Delta_0^2$. Therefore, $d^2_{\text{SP-I}}(\text{free}) = \min\{d^2_{1(\text{SP-I})}, d^2_{2(\text{SP-I})}\} = \min\{4, 2 + 2\Delta_0^2\}$ and $d^2_{\text{SP-II}}(\text{free}) = \min\{d^2_{1(\text{SP-II})}, d^2_{2(\text{SP-II})}\} = \min\{4, 4\Delta_0^2\}$.

For the 8PSK scheme $d^2_{(\text{SP-I})}(\text{free}) = d^2_{2(\text{SP-I})} = 3.17$ while $d^2_{(\text{SP-II})}(\text{free}) = d^2_{2(\text{SP-II})}2.34$ (a loss of 1.315 dB). For the 2FSK/4PSK scheme, $d^2(\text{free})$ depends on Δ_0^2. If $\Delta_0^2 < 1$, $d^2_{2(\text{SP-I})} < d^2_{1(\text{SP-I})}$, hence $d^2_{(\text{SP-I})}(\text{free}) = 2 + 2\Delta_0^2$; $d^2_{2(\text{SP-II})} < d^2_{1(\text{SP-II})}$, hence $d^2_{(\text{SP-II})}(\text{free}) = 4\Delta_0^2$. Since $d^2_{(\text{SP-II})}(\text{free}) < d^2_{(\text{SP-I})}(\text{free})$, two separate designs are needed for the AWGN channel and the fading channel. If $\Delta_0^2 \geq 1$, $d^2_{1(\text{SP-I})} \leq d^2_{2(\text{SP-I})}$ and $d^2_{(\text{SP-I})}(\text{free}) = 4$; similarly, $d^2_{1(\text{SP-II})} \leq d^2_{2(\text{SP-II})}$ and $d^2_{2(\text{SP-II})}(\text{free}) = 4$. Thus, for $\Delta_0^2 \geq 1$, i.e., $h \geq 0.5$, the fading channel design SP-II simultaneously satisfies the $d^2(\text{free})$, $L_{\min}$ and P criteria.

For the four-state fully connected trellis (i.e., transitions emanating from one state go to all other states in the trellis), eight subsets are required. These subsets are obtained by an odd-even split of the elements in the subsets of Fig. 3. However, since the values of $d^2_{1(\text{SP-I})}$ and $d^2_{1(\text{SP-II})}$ remain equal to 4.0, no further coding gains accrue.

For the eight-state fully connected trellis, with a further division of subsets, $d^2_{1(\text{SP-I})} = d^2_{1(\text{SP-II})} = 8.0$. Then $d^2_{(\text{SP-I})}(\text{free}) = \min\{8, 2\Delta_0^2 + 2\}$, and $d^2_{(\text{SP-II})}(\text{free}) = \min\{8, 4\Delta_0^2\}$. For $\Delta_0^2 \geq 1$, $d^2_{(\text{SP-II})}(\text{free}) \geq d^2_{(\text{SP-I})}(\text{free})$, and SP-II simultaneously meets the $d^2(\text{free})$, $L_{\min}$ and P criteria. Note that for $\Delta_0^2 = 2$, $d^2_{(\text{SP-II})}(\text{free})$ is determined by the error event with $d^2(0,4) + d^2(0,2) = 6.0$. This error event is due to signals within the same MPSK subset and is independent of h.

For the eight state trellis, $d^2(\text{free})$ is not determined by the distance between the parallel transitions. Therefore, consider a 16-state half-connected trellis (i.e., transitions emanating from each state go to only half the total number of trellis states). For this trellis,

$$\begin{aligned} d^2_{(\text{SP-I})}(\text{free}) &= \min\{8, 2\Delta_0^2 + 4\} && \Delta_0^2 < 1 \\ &= \min\{8, 2 + 4\} && \Delta_0^2 \geq 1 \\ d^2_{(\text{SP-II})}(\text{free}) &= \min\{8, 6\Delta_0^2\} && \Delta_0^2 < 1 \\ &= \min\{8, 2\Delta_0^2 + 4\} && \Delta_0^2 \geq 1. \end{aligned}$$

Again, for $\Delta_0^2 \geq 1$, SP-II simultaneously meets the $d^2(\text{free})$, $L_{\min}$, and P criteria.

Thus, it may be concluded that for MTCM/(2FSK/4PSK) schemes with $\Delta_0^2 \geq 1$, SP-II is optimum for both the AWGN channel and for the fading channel. In this paper, the analysis of MTCM/(2FSK/4PSK) is carried out for values of h giving $\Delta_0^2 \geq 1$, i.e., $h \geq 0.5$, and consequently using SP-II only. The performance of MTCM/8PSK is discussed with both designs, SP-I and SP-II.

The calculation of upper bounds to $d^2(\text{free})$ may be carried out by using pair-state transition diagrams, and the generalized transfer function technique proposed by Biglieri in [9] for conventional TCM systems. A plot of the squared free distance versus h ($0.5 \leq h \leq 1.0$) with 0° and 45° phase shift, for the eight-state trellis is shown in Fig. 4. The similarity between the two sets of curves in Fig. 4 and Fig. 2, reflects the influence of Δ_0^2 on $d^2(\text{free})$.

The values of $d^2(\text{free})$ and P for the MTCM/(2FSK/4PSK) scheme for selected values of h and ϕ ($= (\pi/M)°$ for 2FSK/MPSK schemes), and for the MTCM/8PSK scheme are illustrated in Table III as well as in Table II. Due to the presence of parallel transitions in the trellis, the length $L_{\min}$ is equal to 2 for both schemes.

Comparing the two modulation schemes, it may be concluded that MTCM/(2FSK/4PSK) provides coding gains (versus MTCM/8PSK) in $d^2(\text{free})$ for both the SP-I and SP-II designs of the latter, and consequently outperforms it on the AWGN channel. For the two-state trellis, and $h =$

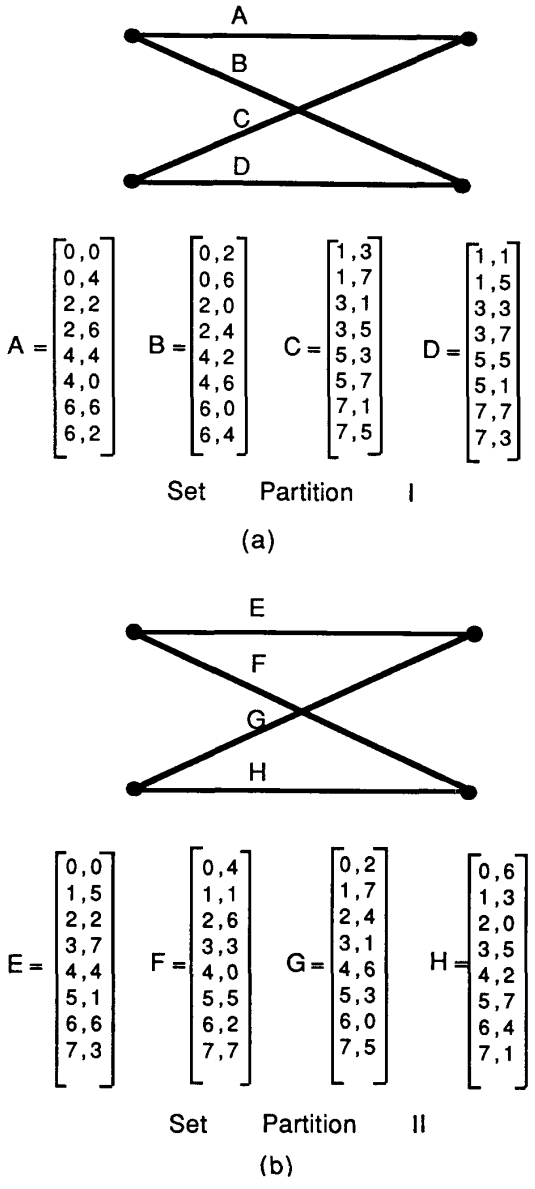

Fig. 3. Two-state trellis codes for the rate $4/6$ MTCM scheme ($k = 2$) with (a) Set Partition I (SP-I) and (b) Set Partition II (SP-II).

$0.5\,(\phi = 45°)$, the larger $d^2(\text{free})$ results in a coding gain of $10\log_{10} 4/3.17 = 1.01$ dB. Note that the SP-II design of MTCM/8PSK carries a penalty of 1.315 dB dut to the lower value of $d^2(\text{free})$ when compared to the SP-I design as previously noted in [6]. For the 16-state trellis, with $h = 1$, the coding gain due to $d^2(\text{free})$ is $10\log_{10} 8/5.17 = 1.9$ dB versus MTCM/8PSK (with the SP-I design). Coding gains are also observed for the four-state and the eight state trellises.

As far as the performance on the fading channel is concerned, the MTCM/(2FSK/4PSK) scheme provides a larger value of P versus MTCM/8PSK, only for the two-state trellis. This improvement corresponds to a coding gain in the range of 1.02 dB (for $h = 0.5$, $\phi = 45°$) to

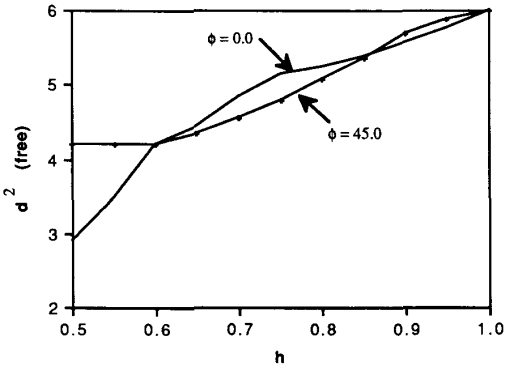

Fig. 4. $d^2(\text{free})$ versus h for the 2FSK/4PSK signal set with 0° and 45° phase shift, for the eight-state trellis code of the rate $4/6$ MTCM scheme ($k = 2$) with Set Partition I.

2.39 dB (for $h = 1.0$, $\phi = 0°$) on the Rayleigh-fading channel, and from $10\log_{10}\left(P_{(2\text{FSK}/4\text{PSK})}/P_{(8\text{PSK})}\right)^{1/2L} = 10\log_{10}(3.2/2)^{1/4} = 0.51$ dB (for $h = 0.5$, $\phi = 45°$) to 1.19 dB (for $h = 1.0$, $\phi = 0°$) on the one-sided normal fading channel. Further gains on the fading channel with $\gamma > 0$ result due to the additional contribution from the increased $d^2(\text{free})$.

When MTCM/FPM is compared to TCM/FPM, coding gains are observed for the two-state trellis due to the increased values of $d^2(\text{free})$ [for example, with $h = 0.5$, $\phi = 45°$ the gain is $10\log_{10} 4/3.1 = 1.11$ dB]. Larger gains are obtained with increasing values of h. For the 16-state trellis the increased value of $d^2(\text{free})$ for $h = 1.0$, yields a gain of 1.25 dB. Coding gains are not observed for the four-state and the eight-state trellises. On the fading channel, the higher multiplicity of the MTCM scheme ($L_{\min} = 2$) ensures better asymptotic performance compared to it's TCM counterpart ($L_{\min} = 1$ for conventional TCM with parallel transitions in the trellis).

Fig. 5 contains plots of the pairwise error probability upper bound[3] ([5, eq. (4)]) versus SNR $(\overline{E}_s/N_0)$ for the two-state rate $4/6$ MTCM/(2FSK/4PSK) scheme ($h = 0.5$, $\phi = 45°$) and the MTCM/8PSK scheme using SP-II [6]. For the MTCM/8PSK scheme, the one-branch (parallel) error event path has the length $L_{\min} = 2$ and $P = 2.0$. The $d^2(\text{free})$ ($= 2.34$) of this scheme is determined by the two-branch error event path with $L = 4(> L_{\min})$. The curves drawn are for the error events along the one-branch path and the two-branch path. For this scheme, at $\gamma = 0$, the performance is dominated exclusively by the one-branch error event. At $\gamma = 10$, the one-branch error event dominates the performance only in the upper SNR range. As γ increases, the SNR at which the one-branch error event begins to dominate the performance also increases. For the MTCM/(2FSK/4PSK) scheme, the one-branch error event path has the length $L_{\min} = 2$ and $P = 3.2$. The $d^2(\text{free})$ $(= 4.0)$ of this scheme is also determined by the one-branch error event path. The performance is determined by the single curve drawn to represent the probability of this error event, at all values of γ. The gain of 1.02 dB (due to the higher value of P) obtained by

[3] Note that the bound of [5, eq. (4)] derived for MTCM/MPSK is also valid for MTCM/FPM when the appropriate squared Euclidean distances are used.

TABLE III
d^2(free) AND P FOR MTCM/(2FSK/4PSK) AND MTCM/8PSK

	$h = 0.5,\ \phi = 45°$		$h = 0.75,\ \phi = 0°$		$h = 1.0,\ \phi = 0°$		8PSK[a]
N	d^2(free)	P	d^2(free)	P	d^2(free)	P	P
2	4.0	3.2	4.0	3.8	4.0	4.0	2.0
4	4.0	4.0	4.0	4.0	4.0	4.0	4.0
8	4.2	16.0	5.1	16.0	6.0	16.0	16.0
16_{HC}	6.2	16.0	7.2	16.0	8.0	16.0	16.0

[a]Refer Table II for d^2(free) for the 8PSK scheme.

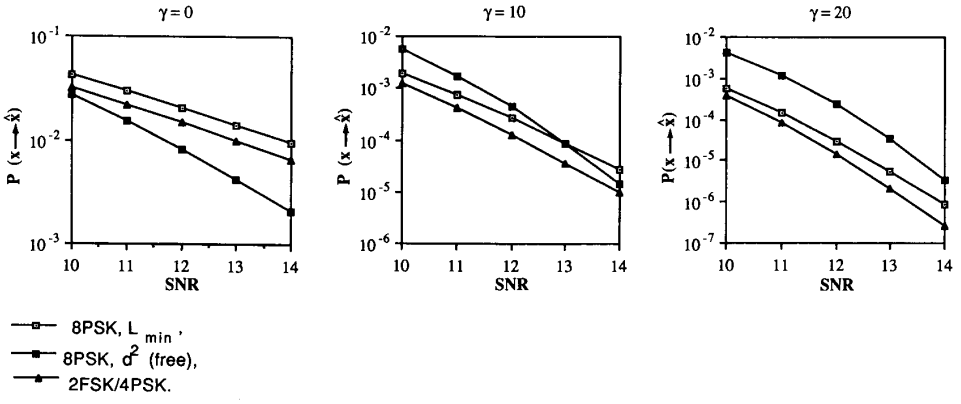

Fig. 5. Pairwise error probability versus SNR at various values of γ for the MTCM/(2FSK/4PSK) scheme ($h = 0.5, \phi = 45°$), and the MTCM/8PSK scheme.

the MTCM/(2FSK/4PSK) scheme at $\gamma = 0$, increases further with higher values of γ, due to the contribution of the increased d^2(free). At $\gamma = \infty$, the gain will be due to the higher d^2(free) alone ($= 10\log_{10} 4/2.34 = 2.33$ dB).

In practical systems (e.g., with nonideal equalizers), where residual fading effects influence the performance (assuming ideal interleaving/deinterleaving), the fading parameter γ may be sufficiently large, and the performance may be guided by the error event path with length greater than $L_{\min}$, as discussed in the previous paragraph. Alternately, in systems with no interleaving/deinterleaving, the performance is determined by d^2(free) [5]. Under either of the two circumstances mentioned above, the MTCM/(2FSK/4PSK) scheme is expected to perform better than the MTCM/8PSK scheme (refer to Tables II and III for values of d^2(free) and P). The 2FSK/4PSK scheme using two 4PSK constellations has an additional advantage over the 8PSK scheme with respect to phase jitter sensitivity.

B. MTCM/(2FSK/8PSK)

The 2FSK/8PSK signal set is used in conjunction with the rate 5/8 trellis encoder. The signal assignments to the two-state trellis for optimum performance on the fading channel (SP-II) are shown in Fig. 6. The values of d^2(free) and P are listed in Table IV for the MTCM(2FSK/8PSK) scheme with $h = 0.5$ ($\phi = 22.5°$), and for the MTCM/16PSK scheme with set partitionings SP-I and SP-II. Again, when applied to MTCM/FPM, SP-II is observed to meet the design criteria for the AWGN channel and the fading channel. For the two-state trellis, the gain in d^2(free) over MTCM/16PSK is $10\log_{10} 2.34/1.476 = 2.0$ dB. The larger value of P for the MTCM/(2FSK/8PSK) scheme yields a gain of $10\log_{10}(1.246/0.188)^{1/2} = 4.11$ dB on the Rayleigh-fading channel, and 2.05 dB on the one-sided normal fading channel. With increasing h, the gain in d^2(free) is limited to 2.0 dB by the distances for the 8PSK signal set at the two FSK frequencies. For this scheme with non-integer throughput of 2.5 bps/Hz, there is no equivalent TCM/FPM scheme.

IV. DISCUSSION

FPM signal sets have the advantage of providing higher values of Δ_0^2 when compared to their equivalent MPSK signal sets (for $M > 4$).[4] In the analysis of MTCM/FPM with $h \geq 0.5$, it is observed that the set partitioning designed to maximize symbol diversity (asymptotically optimum for the Rayleigh fading channel) provides asymptotically optimum performance on the AWGN channel as well. When compared to MTCM/MPSK, coding gain due to d^2(free) results in improved performance on the AWGN channel and on the Rician fading channel with $\gamma > 0$. When an improvement in the value of P occurs (e.g., the two-state MTCM/FPM scheme), MTCM/FPM performs better than MTCM/MPSK on the Rician-fading channel ($\gamma < \infty$), and on the one-sided normal fading channel.

[4]It is not practical to use a 2FSK/2PSK signal set in place of a 4PSK signal set, because Δ_0^2 of the 4PSK signal set is equal to 2.0, and the maximum value of Δ_0^2 achievable with 2FSK/MPSK signal sets is also equal to 2.0. Therefore, the use of the latter set in place of the former will not provide any coding gains.

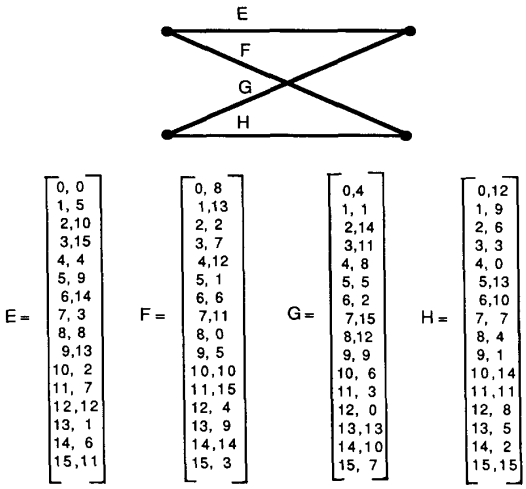

Fig. 6. Two-state trellis code for the rate 5/6 MTCM ($k = 2$, 16-ary signals) with Set Partition II.

TABLE IV
d^2(free) AND P FOR MTCM/(2FSK/8PSK) AND MTCM/16PSK

	2FSK/8PSK $h = 0.5$, $\phi = 22.5°$			16PSK		
	SP-I	SP-II		SP-I	SP-II	
S	d^2(free)	d^2(free)	P	d^2(free)	d^2(free)	P
2	2.00	2.34	1.25	1.48	1.39	0.19
4	2.34	2.34	2.00	1.48	1.48	2.00
8_{HC}	2.34	3.51	2.00	2.34	2.56	2.0

While making the comparison with MTCM/MPSK, it is important to consider the bandwidth expansion of FPM schemes over MPSK schemes. The FPM schemes require a greater 90% bandwidth (band of frequency containing 90% of the total signal power) than MPSK schemes [10], but the bandwidth occupancy is found to be lower than that of MPSK schemes at several other values[5] of the percentage signal power. The complexity of the two schemes is the same, since the only difference between the two schemes is in the choice of signal sets (FPM or MPSK).

The MTCM/FPM schemes discussed in this paper also have to be compared to their conventional TCM counterparts for which FPM was proposed [10]. On the AWGN channel, the MTCM/(2FSK/4PSK) scheme yields performance gains over the TCM/(2FSK/4PSK) scheme for the two-state trellis and for the 16-state trellis. On the fading channel, the MTCM/FPM schemes are superior to the TCM/FPM schemes due to the larger value of signal diversity obtained by them for the two-state trellis. Again, when the number of states is large enough that there are no parallel transitions in the MTCM trellis, the signal diversity is more than that obtainable by conventional TCM schemes. This behavior on the AWGN channel and on the fading channel is consistent with that observed for MTCM/MPSK with respect to TCM/MPSK. It must be pointed out that in cases where MTCM trellises have parallel transitions and the equivalent TCM trellises have none, the TCM scheme may be preferred. Compare the eight-state rate 2/3 TCM/8PSK scheme $\left(d^2(\text{free}) = 4.586,\ L_{\min} = 3\right)$ to the eight-state rate 4/6 MTCM/8PSK scheme $\left(d^2(\text{free}) = 3.17,\ L_{\min} = 2\right)$. Similar conclusions hold for the FPM signal sets as well.

In the comparison of MTCM/FPM to TCM/FPM, since both schemes employ FPM signals, the bandwidth occupancy is not the issue, but the complexity is. The normalized complexity per 2-D signal is defined as $c = 2^{\tilde{b}+v}/k$ [6], where $\tilde{b}$ is the number of encoded bits, 2^v is the number of states, and k is the code multiplicity. Here, $\tilde{b}$ defines the connectivity of the trellis (i.e., the number of states to which a given state in the trellis is connected). For a given number of states and trellis connectivity, the complexity of the MTCM scheme is equal to $1/k$ times the complexity of the TCM scheme. Therefore, MTCM schemes have a lower normalized complexity per 2-D signal. This description of complexity ignores the aspect of subset decoding. Indeed, for MTCM schemes, the size of the subsets (signals assigned to parallel transitions in the trellis) is

[5]It has been shown that the bandwidth occupancy of FPM schemes is lower than that of MPSK schemes at (among other values) 91, 95.5, and 99% of total signal power [15]. With respect to the MPSK signal bandwidth occupancy, the 90% bandwidth for $h = 0.5$ and 1.0 is 1.35 and 1.2 times, respectively, while the 91% bandwidth for the same values of h is reduced to 0.95 and 0.9 respectively.

larger than that for TCM schemes. For example, for the two-state rate $2/3$ TCM and rate $4/6$ MTCM ($k = 2$) schemes the number of parallel transitions (i.e., the size of the subset) equals 2 and 8 respectively. Therefore, the subset decoding complexity of MTCM schemes is higher than that of TCM schemes. This issue has been addressed in detail in [16].

The significance of the simultaneous optimization of the design criteria for the AWGN channel and the fading channel is evident in Fig. 5. In this figure, the performance gain of MTCM/(2FSK/4PSK) over MTCM/8PSK for the two-state trellis, increases with increasing values of γ due to the additional contribution of the larger $d^2(\text{free})$ to the gain obtained on the Rayleigh-fading channel due to the increased value of P.

The Nakagami-m fading model and the Rician-fading model were both proposed as generalizations of the Rayleigh fading model. The performance analysis of trellis codes on the fully interleaved (zero memory) nonselective fading channel, using the Nakagami-m fading model as an alternative to the Rician-fading model, results in a simple expression for the error probability upper bound. The analysis of this expression is useful in revealing the likenesses and disparities of the two "suggested equivalent" fading models. For the extreme cases of Rayleigh fading and AWGN (no fading), the upper bound agrees perfectly with the results obtained using the Rician-fading model. For intermediate cases of fading, an examination of the asymptotic expressions for the pairwise error probabilities for the two fading models reveals that the bounds are equivalent only at low SNR's with the disparity becoming considerable at high SNR's. The disparity is due to the diversity introduced by the channel in the asymptotic expression for the pairwise error probability calculated with the Nakagami-m fading model. In this paper, the performance analysis on the Rician-fading channel is carried out by using [5, eq. (4)].

The special case of one-sided normal fading is represented by the Nakagami-m fading model with $m = 1/2$. For this channel, it is shown that the trellis code design parameters are the same as those for the Rayleigh-fading channel.

ACKNOWLEDGMENT

The authors would like to thank Dr. M. K. Simon for pointing out the paper by P. Crepeau [14]. The authors are indebted to the anonymous reviewers whose constructive remarks have improved the quality of this paper.

REFERENCES

[1] G. Ungerboeck, "Trellis-coded modulation with redundant signal sets part II: State of the Art", *IEEE Commun. Mag.*, vol. 25, pp. 12–21, Feb. 1987.
[2] G. D. Forney, R. G. Gallager, G. R. Lang, F. M. Longstaff, and S. U. Qureshi, "Efficient modulation for band-limited channels," *IEEE Trans. J. Select. Areas Commun.*, vol. SAC-2, pp. 632–647, Sept. 1984.
[3] L. F. Wei, "Trellis-coded modulation with multidimensional constellations," *IEEE Trans. Inform. Theory*, vol. IT-33, pp. 483–501, July 1987.
[4] D. Divsalar and M. K. Simon, "Multiple trellis coded modulation," *IEEE Trans. Commun.*, vol. 36, pp. 410–419, Apr. 1988.
[5] ——, "The design of trellis coded MPSK for fading channels: Performance criteria," *IEEE Trans. Commun.*, vol. 36, pp. 1004–1012, Sept. 1988.
[6] ——, "The design of trellis coded MPSK for fading channels: Set partitioning for optimum code design," *IEEE Trans. Commun.*, vol. 36, pp. 1013–1021, Sept. 1988.
[7] ——, "Generalized multiple trellis coded modulation (MTCM)," in *IEEE Global Telecommun. Conf. Rec.*, Tokyo, Japan, Nov. 1987.
[8] G. Ungerboeck, "Channel coding with multilevel phase signals," *IEEE Trans. Inform. Theory*, vol. IT-28, pp. 55–67, Jan. 1982.
[9] E. Biglieri, "High-level modulation and coding for nonlinear satellite channels," *IEEE Trans. Commun.*, vol. COM-32, pp. 616–626, May 1984.
[10] R. Padovani and J. K. Wolf, "Coded phase/frequency modulation," *IEEE Trans. Commun.*, vol. COM-34, pp. 446–453, May 1986.
[11] M. Nakagami, "The m-distribution—A general formula of intensity distribution of rapid fading," in *Statistical Methods of Radio Wave Propagation*, Ed. W. C. Hoffman, Ed. New York: Pergamon, 1960, pp. 3–36.
[12] D. Divsalar and M. K. Simon, "Trellis coded modulation for 4800 to 9600 bps transmission over a fading satellite channel," *IEEE J. Select. Areas Commun.*, vol. SAC-5, pp. 162–175, Feb. 1987.
[13] I. S. Gradshteyn and I. M. Ryzhik, *Tables of Integrals Series and Products*. New York: Academic, 1965.
[14] P. J. Crepeau, "Coding performance on generalized fading channels," *IEEE MILCOM 1988*, San Diego, CA, pp. 15.1.1–15.1.7.
[15] S. Qu *Oral Communication.*
[16] S. S. Pietrobon, R. H. Deng, A. Lafanachere, G. Ungerboeck, and D. J. Costello, "Trellis-coded multidimensional phase modulation," *IEEE Trans. Inform. Theory*, vol. 36, pp. 63–89, Jan. 1990.

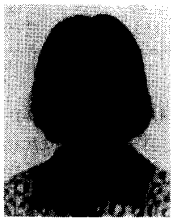

Shalini S. Periyalwar received the B. Eng. degree in electrical engineering from Bangalore University, India, in 1981. Since 1985, she has been with the Technical University of Nova Scotia, Halifax, Canada, where she completed the M.A.Sc. degree in 1987. She is currently in the Ph.D. program in Electrical Engineering. Her thesis is in the area of trellis coded modulation.

Her current research interests are in the area of coding and modulation for fading channels.

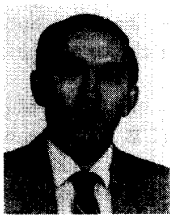

Solomon M. Fleisher (M'72–SM'80) received the M.S. and Ph.D. degrees from the Institute of Communications Engineering, Leningrad, U.S.S.R., in 1954 and 1965, respectively.

From 1954 to 1962 he worked on the design of the high-fidelity broadcast receivers in Riga, Latvia. In 1962 he joined the Institute of Communications Engineering, Leningrad, where he was (from 1968) an Associate Professor. In 1972 he joined the Ben-Gurion University, Beersheva, Isreal, and in 1975 the Holon Institute of Technology, Tel-Aviv University. Since 1982 he has been Professor of Electrical Engineering at the Technical University of Nova Scotia, Halifax, Canada. He spent the 1977–1978 academic year with the University of Manitoba, Winnipeg, Canada, the summer of 1979 with the Institute of Telecommunications at the Swiss Federal Institute of Technology, Zurich, the 1981–1982 academic year with the Technical University of Nova Scotia, and part of the 1990–1991 academic year with the University of Toronto. His current research interests include coded modulation and communication theory.